Targeting Elastase for Molecular Imaging of Early Atherosclerotic Lesions

Almut Glinzer,* Xiaopeng Ma,* Jaya Prakash, Melanie A. Kimm, Fabian Lohöfer, Katja Kosanke, Jaroslav Pelisek, Moritz P. Thon, Sandra Vorlova, Katrin G. Heinze, Hans-Henning Eckstein, Michael W. Gee, Vasilis Nitziachristos, Alma Zernecke,* Moritz Wildgruber*

Objective—Neutrophils accumulate in early atherosclerotic lesions and promote lesion growth. In this study, we evaluated an elastase-specific near-infrared imaging agent for molecular imaging using hybrid fluorescence molecular tomography/x-ray computed tomography.

Approach and Results—Murine neutrophils were isolated from bone marrow and incubated with the neutrophil-targeted near-infrared imaging agent Neutrophil Elastase 680 FAST for proof of principle experiments, verifying that the elastase-targeted fluorescent agent is specifically cleaved and activated by neutrophil content after lysis or cell stimulation. For in vivo experiments, low-density lipoprotein receptor–deficient mice were placed on a Western-type diet and imaged after 4, 8, and 12 weeks by fluorescence molecular tomography/x-ray computed tomography. Although this agent remains silent on injection, it produces fluorescent signal after cleavage by neutrophil elastase. After hybrid fluorescence molecular tomography/x-ray computed tomography imaging, mice were euthanized for whole-body cryosectioning and histological analyses. The in vivo fluorescent signal in the area of the aortic arch was highest after 4 weeks of high-fat diet feeding and decreased at 8 and 12 weeks. Ex vivo whole-body cryoslicing confirmed the fluorescent signal to locate to the aortic arch and to originate from the atherosclerotic arterial wall. Histological analysis demonstrated the presence of neutrophils in atherosclerotic lesions.

Conclusions—This study provides evidence that elastase-targeted imaging can be used for in vivo detection of early atherosclerosis. This imaging approach may harbor potential in the clinical setting for earlier diagnosis and treatment of atherosclerosis. **(*Arterioscler Thromb Vasc Biol*. 2017;37:00-00. DOI: 10.1161/ATVBAHA.116.308726.)**

Key Words: arteriosclerosis ■ cardiovascular disease ■ fluorescence molecular tomography ■ imaging ■ neutrophils

Cardiovascular disease is the most common cause of mortality in the industrialized world and represents 31% of global deaths.[1] Atherosclerosis is regarded as a chronic inflammatory disease of the arterial wall, manifesting in cardiovascular events, such as myocardial infarction or stroke. Hypercholesterolemia, hypertension, and cigarette smoking are the most common risk factors of atherosclerosis and accelerate the inflammatory process.[2,3]

Damage or dysfunction of the endothelium is considered a critical event triggering atherosclerosis, leading to an increased permeability for substances, such as low-density lipoproteins, and an increased adhesiveness for leukocytes. Within the arterial intima, lipoproteins undergo oxidative modifications and are internalized by monocytes, which differentiate into macrophage foam cells. The local inflammatory response is furthermore sustained by activation of smooth muscle cells and influx of additional immune cells, which together with macrophages release various cytokines and mediators supporting the inflammatory cascade.

Besides macrophages that are considered key players in the formation of atherosclerotic lesions, it was recently shown that neutrophils also play an important role in atherosclerosis, in particular, during early stages of lesion formation.[4–7] As part of the innate immune system, neutrophils are usually recruited for first-line defense against invading pathogens that are attacked by phagocytosis and neutrophil-specific effector molecules released by degranulation, such as myeloperoxidase, neutrophil elastase, cathepsin G, and proteinase 3.[8]

Received on: June 14, 2016; final version accepted on: December 21, 2016.

From the Institut für diagnostische und interventionelle Radiologie, Klinikum rechts der Isar (A.G., M.A.K., F.L., K.K., M.W.), Klinik für vaskuläre und endovaskuläre Chirurgie, Klinikum rechts der Isar (A.G., J. Pelisek, H.-H.E.), Mechanics & High Performance Computing Group (M.P.T., M.W.G.), and Chair of Biological Imaging, Klinikum Rechts der Isar (V.N.), Technische Universität München, Germany; Institute for Biological and Medical Imaging, Helmholtz Zentrum München, Neuherberg, Germany (X.M., J. Prakash, V.N.); Institut für Experimentelle Biomedizin, Universitätsklinikum Würzburg, Germany (S.V., A.Z.); Rudolf Virchow Zentrum, Universität Würzburg, Germany (K.G.H.); and Translational Research Imaging Center, Universitätsklinikum Münster, Germany (M.W.).

*These authors contributed equally to this article.

The online-only Data Supplement is available with this article at http://atvb.ahajournals.org/lookup/suppl/doi:10.1161/ATVBAHA.116.308726/-/DC1.

Correspondence to Moritz Wildgruber, MD, PhD, Translational Radiology Research Imaging Center (TRIC), Institut für Klinische Radiologie, Universitätsklinikum Münster, Westfälische Wilhelms Universität, Albert-Schweitzer-Campus 1, Gebäude A1, D-48149 Münster, Germany. E-mail moritz.wildgruber@ukmuenster.de

Nonstandard Abbreviations and Acronyms	
FMT	fluorescence molecular tomography
HFD	high-fat diet
NIRF	near-infrared fluorescence
XCT	x-ray computer tomography

Neutrophils and their effector molecules have been identified in murine and human atherosclerotic plaques by immunohistochemistry and fluorescence techniques, such as flow cytometry and confocal microscopy.[4,6,7,9–11] Functionally, it has been demonstrated that neutrophils accumulate within atherosclerotic vessels, in particular, during early plaque formation and secret preformed granule proteins, which may instruct recruitment and activation of other inflammatory cells[12] to promote atherosclerotic lesion formation.

Extracellular proteolytic processes modulate plaque stability. Breakdown of extracellular matrix by matrix metalloproteinases and cathepsins can increase the vulnerability of the plaque, rendering it prone to rupture, a mechanism that can trigger sequelae, such as myocardial infarction or stroke. Neutrophil elastase in this process additionally contributes to matrix degradation and weakening of the vessel wall.[13]

Preclinical imaging technologies enable novel insights into cardiovascular diseases because they can depict the dynamic expression of biomarkers during disease development. Fluorescence molecular imaging has emerged as a powerful tool because it can target multiple biological aspects of the disease by using high-affinity ligands labeled with near-infrared fluorochromes that are directed toward key cellular and molecular players of atherosclerosis.[14] Fluorescence molecular tomography (FMT) fused with x-ray computer tomography (XCT) cannot only detect but also quantify inflammatory processes in atherosclerotic lesions dynamically in vivo and over time.[14–16]

To date, molecular imaging has primarily focused on the detection of monocytes/macrophages and their effector molecules, such as cathepsins and matrix metalloproteinases. Molecular imaging of neutrophils as early contributors to atherosclerotic lesion formation and elastase as its major effector is expected to be challenging. Neutrophils have a short life span and undergo rapid functional phenotypic changes.[17] In addition, the number of neutrophils and plaque size during early phases of atherosclerosis is limited.[4,7,12,18] Capturing neutrophils or neutrophil elastase noninvasively and in vivo will, therefore, require a technology with adequate sensitivity. However, the possibility to track early stages of atherosclerotic lesion formation in vivo could offer novel insights into the pathophysiology and maturation process. Additionally, it enables the assessment of treatment regimens that aim at targeting atherosclerosis at an early stage, before plaque formation becomes irreversible and plaque rupture can occur.

The aim of our study was, therefore, to investigate neutrophil elastase-targeted FMT for the early assessment of atherosclerotic lesion formation in a murine model of atherosclerosis.

Materials and Methods

Materials and Methods are available in the online-only Data Supplement.

Results

Elastase-Targeted Near-Infrared Fluorescence Agent Is Activated by Isolated Neutrophils in a Concentration-Dependent Manner

We first tested activation of the elastase-specific near-infrared fluorescence (NIRF) agent by neutrophils. To this end, murine neutrophils were isolated from bone marrow and characterized by multicolor flow cytometry. Isolated neutrophils were identified as $CD11b^{+}Ly6G^{+}$ cells within $CD45^{+}$ leukocytes and reached a purity of >90% (Figure 1A).

The NIRF agent can be activated by neutrophil elastase that is usually stored in neutrophil cytoplasmic granules.[19] We, therefore, first analyzed activation of different concentrations of the NIRF agent by lysed neutrophils and could evidence a concentration-dependent increase of emitted fluorescence over time, using both murine and human neutrophils, corresponding to K_m values of 7.3 and 11.2 µmol/L, respectively (Figure 1B and 1C). To further test the specificity of the imaging agent, competition experiments were performed using the selective elastase inhibitor sivelestat[20] with both mouse and human neutrophils. Dose–response curves after inhibition with different concentrations of sivelestat demonstrated effective inhibition of the activation of the NIRF agent (Figure 1D and 1E), as also evident after calculating inhibition curves (Figure 1F and 1G), showing a half maximal inhibitory concentration of 0.9 and 48 nmol/L for murine and human neutrophils, respectively, confirming high specificity of the imaging agent.

In vivo, intracytoplasmatic granules are released from neutrophils on stimulation of the cells. We next assessed activation of the elastase-targeting NIRF agent by neutrophils stimulated with different concentrations of phorbol-12-myristate 13-acetate/ionomycin or N-formyl-Met-Leu-Phe (Figure 2A through 2D). Indeed, the probe was rapidly activated by phorbol-12-myristate 13-acetate/ionomycin-stimulated murine neutrophils in a concentration-dependent manner (Figure 2A), whereas N-formyl-Met-Leu-Phe-activation of murine neutrophils showed less potent activation of the fluorescent probe (Figure 2C). No activation of the probe was detected in unstimulated neutrophils (Figure 2A and 2C). Human neutrophils activated with phorbol-12-myristate 13-acetate/ionomycin generated a fluorescent intensity that was twice as high when compared with murine neutrophils. N-Formyl-Met-Leu-Phe challenging of human neutrophils only marginally increased the fluorescence intensity of the activated probe when compared with nonactivated neutrophils, which served as a control (Figure 2D). Of note, already nonactivated control human neutrophils showed a mild increase of emitted fluorescence when incubated with the NIRF agent over time, which may reflect low levels of spontaneous activation (Figure 2B).

Taken together, the evaluated elastase-targeted fluorescent agent is specifically activated by exposure to both murine and human neutrophil contents after lysis, as well as by activated neutrophils in a concentration-dependent manner.

In Vivo FMT-XCT of Elastase Activity in Atherosclerotic $LDLr^{-/-}$ Mice

The ability of the fluorescent agent to be cleaved and activated in vivo was investigated in atherosclerosis-prone *LDLr*$^{-/-}$ mice

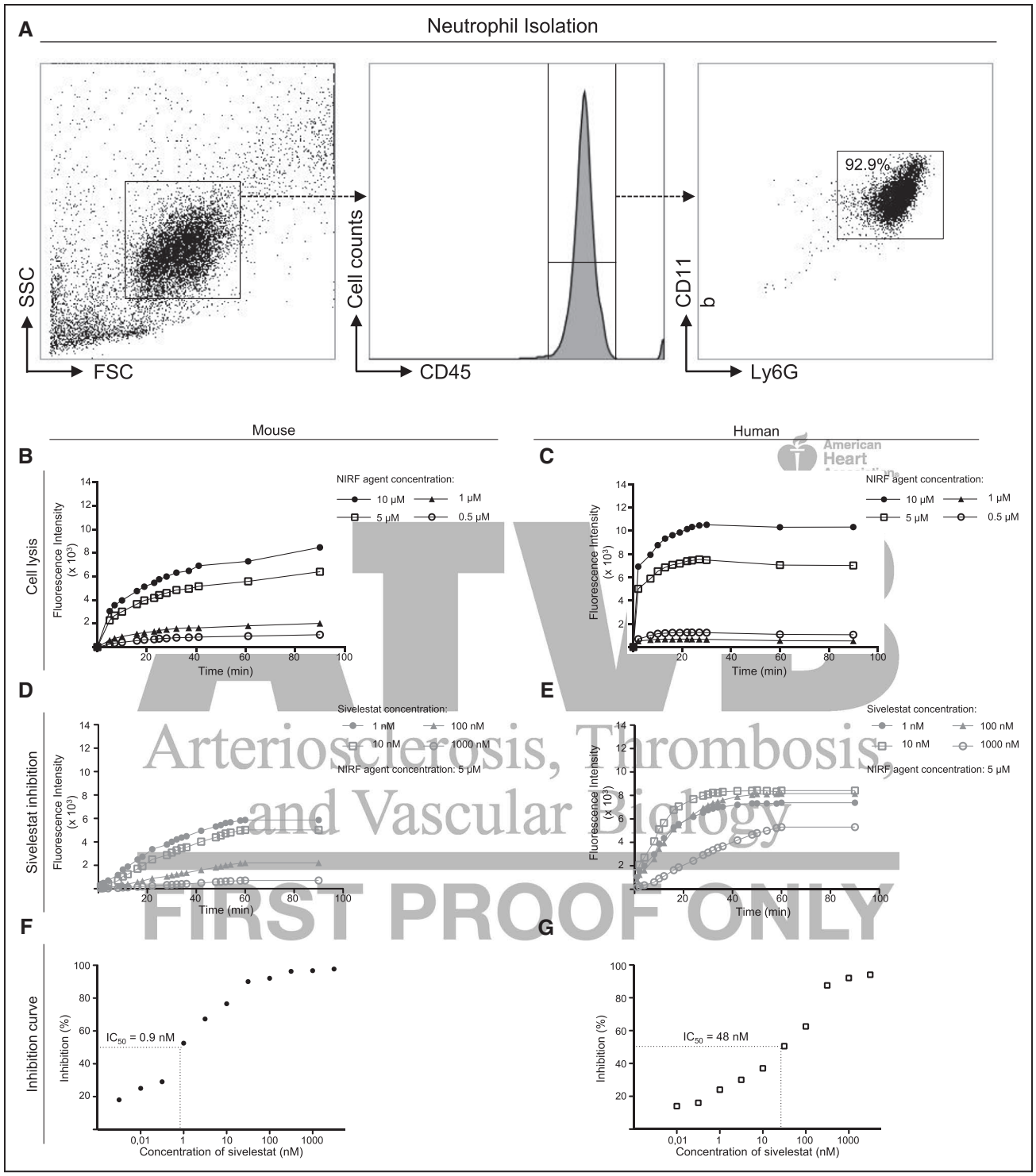

Figure 1. Neutrophil Elastase 680 FAST agent is activated by murine and human neutrophils. **A**, Characterization of neutrophils isolated from murine bone marrow by multicolor flow cytometry. Representative gatings are shown. Neutrophils were identified on their appearance in the forward/sideward scatter (**left**) and staining for CD45 (**central**), Ly6G, and CD11b (**right**). **B** and **C**, Fluorescence intensity (in arbitrary units) of isolated neutrophils incubated with near-infrared fluorescence (NIRF) agent. Murine and human neutrophils were lysed with 0.01% Triton X (**B** and **C**) and incubated with different concentrations of the NIRF imaging agent, showing a concentration dependency. **D–G**, Inhibition experiments with the inhibitor sivelestat demonstrate the specificity of the imaging agent. Enzyme activity after incubation with different concentration of sivelestat was measured over time (**D** and **E**), and the resulting blocking curves are presented (**F** and **G**).

that develop early atherosclerotic lesions in the aortic root and aorta within 4 weeks after start of a high-fat diet (HFD). Mice were put on a HFD for 4, 8, or 12 weeks.[21,22] At each time point, mice were injected with Neutrophil Elastase 680 FAST and imaged by hybrid FMT-XCT. An increased fluorescence signal was observed in atherosclerotic mice after injection

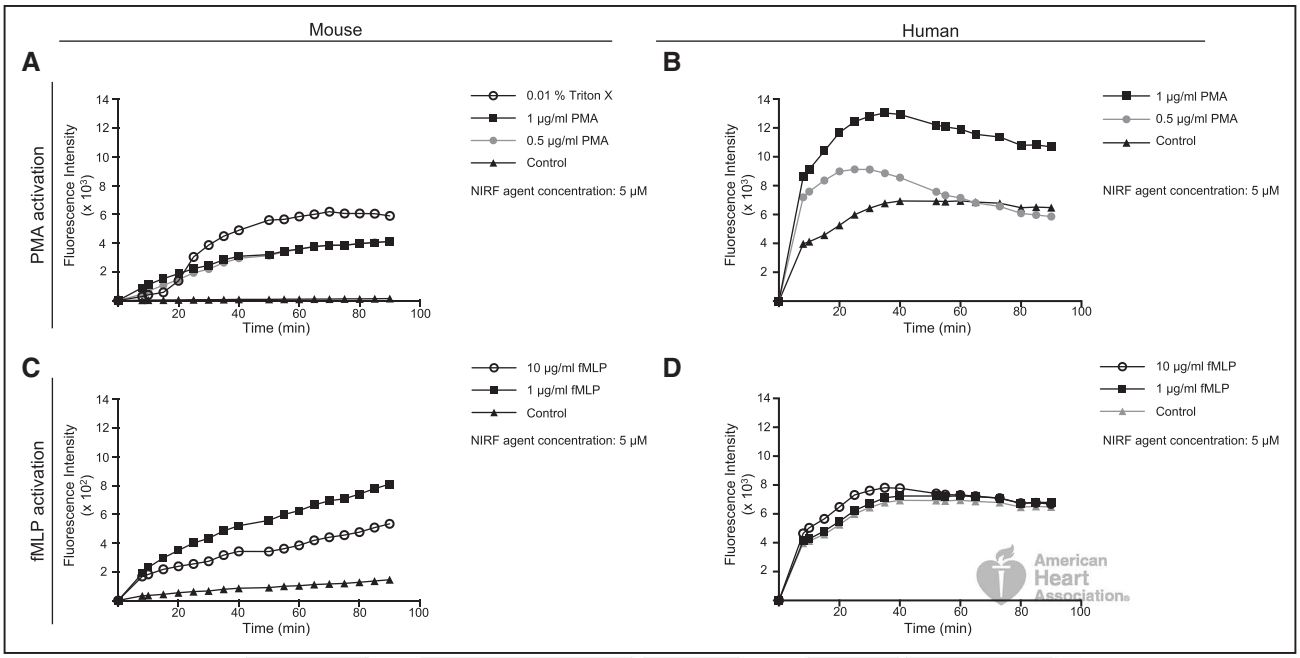

Figure 2. A–D, Elastase release after neutrophil stimulation. Intact cells were stimulated with phorbol-12-myristate 13-acetate (PMA)/ionomycin (**A** and **B**) or N-Formyl-Met-Leu-Phe (fMLP; **C** and **D**) and incubated with 5 µmol/L of the near-infrared fluorescence (NIRF) imaging agent. To compare cell lysis and stimulation, the emitted fluorescence of Triton X lysed cells is shown for PMA activation of murine neutrophils (**C**).

with the elastase-targeted NIRF agent, and hybrid contrast-enhanced XCT enabled colocalization of the fluorescence signal predominantly to the aortic root and arch. Control mice without atherosclerosis showed only weak and unspecific fluorescence signal after injection with the probe (Figure 3A). The mean fluorescence intensity, calculated for the region of interest (root and aortic arch), peaked at 4 weeks of HFD and decreased slightly at 8 and 12 weeks of HFD (Figure 3B). To rule out a major contribution of autofluorescence to this signal, we additionally imaged mice after 4 weeks of HFD without injection of the NIRF contrast agent. However, the captured autofluorescence in these mice proved to be negligible (Figure 3B). Furthermore, mice injected with the NIRF agent before the initiation of HFD, without any atherosclerosis,

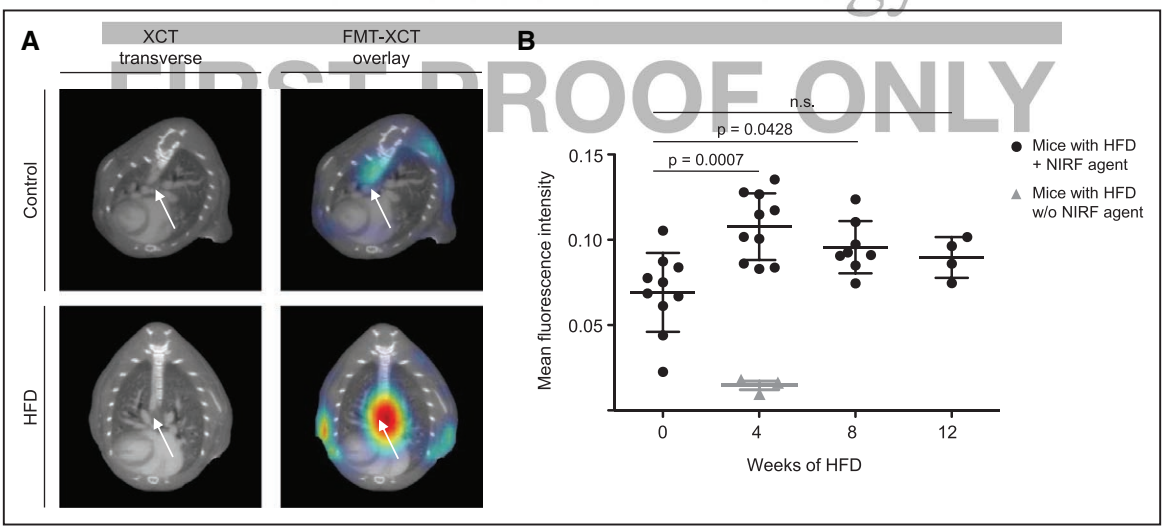

Figure 3. In vivo fluorescence molecular tomography/x-ray computed tomography (FMT-XCT) of elastase activity in the course of atherosclerosis. **A**, In vivo FMT-XCT imaging of control (*LDLr*$^{-/-}$ on normal chow) and atherosclerotic mice (*LDLr*$^{-/-}$ on high-fat diet [HFD]). XCT images (**left**) depict anatomic information. FMT images (**right**) demonstrate elastase activity in vivo 4 h after injection with the near-infrared fluorescence (NIRF) imaging agent. **B**, The mean value of the fluorescence intensity of the region of interest was calculated for each time point, as indicated (0 weeks HFD, n=10; 4 weeks HFD, n=10; 8 weeks HFD, n=8; 12 weeks, HFD n=4). Gray-colored dot plot represents autofluorescence in atherosclerotic mice after 4 weeks of HFD, not injected with the NIRF agent (n=3). Analysis of variance and Bonferroni corrections for multiple comparisons revealed significant differences between fluorescence values at different time points, as indicated (1-way ANOVA, P=0.0012; Bonferroni: 0 vs 4 weeks of HFD, P=0.0007; 0 vs 8 weeks of HFD, P=0.0428; 0 vs 12 weeks of HFD not significant, P=0.4984).

showed only moderate background fluorescence, attributable to unspecific activation within the circulation (Figure 3B).

Fluorescence Elastase Signal in the Aortic Arch Is Confirmed by Whole-Body Cryoslicing

To confirm that the fluorescent signal emitted from the elastase-targeted NIRF agent originates from the aorta of atherosclerotic mice, whole-body cryoslicing was performed, which provides an increased spatial resolution of the emitted fluorescence compared with in vivo FMT. Representative cryoimages of the arch of control and atherosclerotic mice injected with the NIRF agent are shown, as well as images of mice not injected with the probe depicting background autofluorescence (Figure 4A). Fluorescent ratios of the aortic arch were calculated for each time point. Similar to results obtained in vivo, signal intensities in these areas increased after initiating the HFD and peaked at 4 weeks and decreased in the later course of atherosclerosis (Figure 4B). Autofluorescence intensities of mice at 4 weeks of HFD not injected with the NIRF agent were again low (Figure 4B).

Activated NIRF Agent Is Located in the Atherosclerotic Arterial Wall

To further investigate the exact location of the fluorescent signal of the elastase-targeting NIRF agent within the arterial wall, fluorescent microscopy was used. Increased signals in the near-infrared light spectrum (680 nm) were localized to the endothelial cell layer and plaque region in the aortic arch (Figure 4C). In addition, intense near-infrared signal of the elastase-targeting NIRF agent was detected within plaque

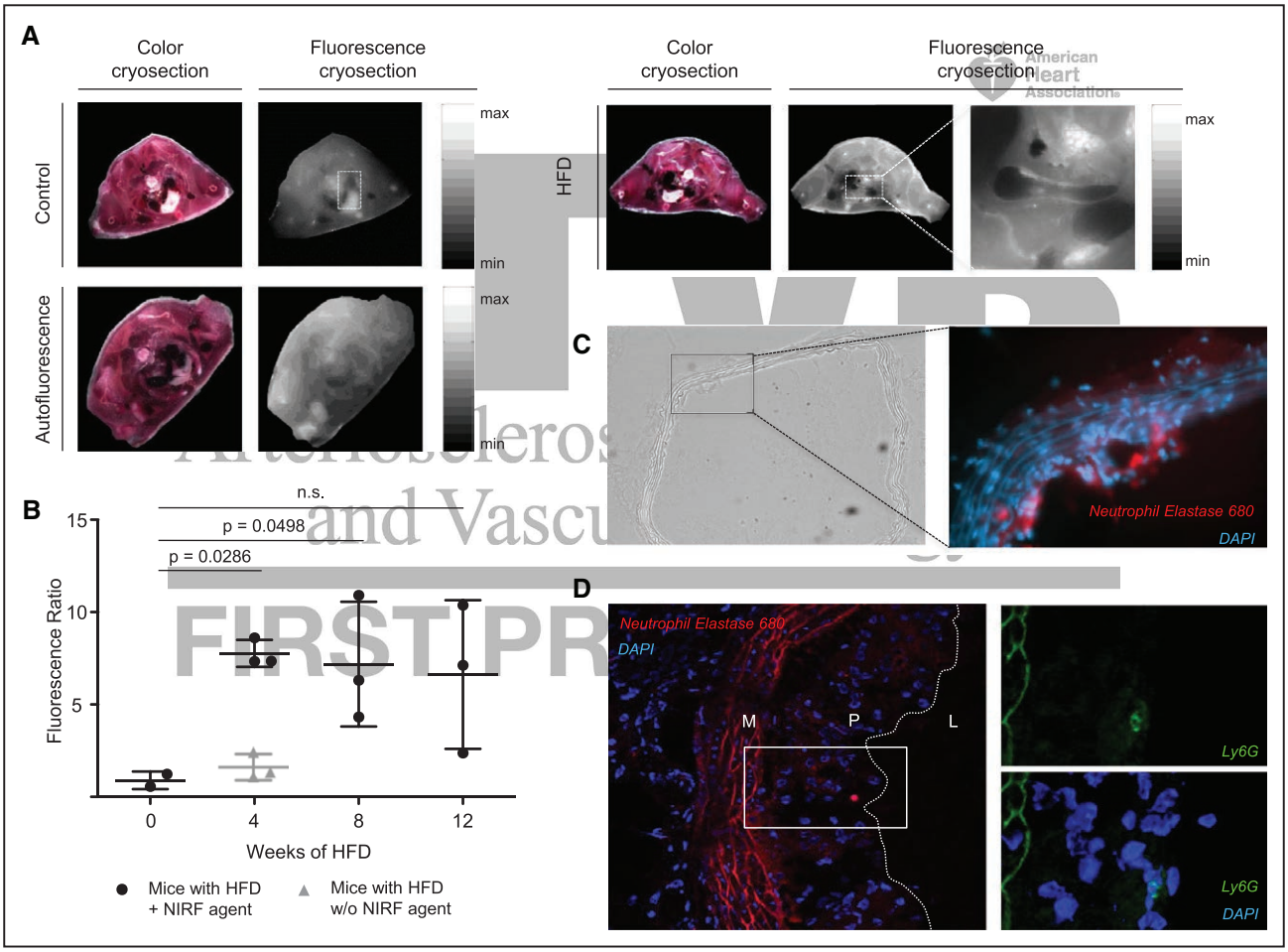

Figure 4. Fluorescence imaging of near-infrared fluorescence (NIRF) imaging agent in whole-body cryosections of atherosclerotic mice. **A**, Representative images of cryosections in the plane of the aortic arch of control (*LDLr*$^{-/-}$ on normal chow) and atherosclerotic mice (*LDLr*$^{-/-}$ on high-fat diet [HFD]), as well as autofluorescence of atherosclerotic mice (mice 4 weeks on HFD not injected with the probe) are shown. **B**, Fluorescence ratio of cryosections calculated of the region of interest (aortic arch; 0 weeks of HFD, n=2; 4 weeks of HFD, n=3; 8 weeks of HFD, n=3; 12 weeks of HFD, n=3). Analysis of variance and Bonferroni corrections for multiple comparisons revealed significant differences between fluorescence ratios at different time points, as indicated (1-way ANOVA, *P*=0.0115; Bonferroni 0 vs 4 weeks of HFD, *P*=0.0286; 0 vs 8 weeks of HFD, *P*=0.0498; 0 vs 12 weeks of HFD not significant, *P*=0.0854). Gray-colored dot plot represents autofluorescence in atherosclerotic mice after 4 weeks of HFD (n=3), not injected with the NIRF agent. **C**, Localization of activated NIRF imaging agent in the ascending aorta. A brightfield image of the atherosclerotic vessel is shown (**left**). A high magnification of the plaque is shown (**right**). The activated imaging agent is represented in red, nuclei are counterstained with DAPI (blue). **D**, Co-localization of activated NIRF imaging agent with neutrophils within atherosclerotic plaques. Localization of the activated NIRF imaging agent (red) within the plaque region (P) in the aortic root of a *Ldlr*$^{-/-}$ mouse fed a HFD for 6 weeks; L indicates lumen; and M, media (**left**). A high magnification of the boxed region depicts immunofluorescence staining for Ly6G (green) in adjacent sections; nuclei are counterstained with DAPI (blue, **right**).

regions in colocalization with Ly6G$^+$ neutrophils, as revealed by confocal microscopy and immunofluorescence staining in adjacent plaque sections of the aortic root (Figure 4D). However, it should be noted that the NIRF signal could also be detected in plaque regions devoid of any Ly6G staining, representing elastase deposits within the atherosclerotic plaque that may have originated from short-lived neutrophils or other cell types.

Histological Analysis of Plaque Size and Neutrophil Counts in Atherosclerotic Lesions

To quantify the progression of atherosclerosis, plaque area was measured in histological sections of the aortic root and aortic arch. Plaque size increased over time in both regions (Figure 5A and 5B). To further localize neutrophils in atherosclerotic lesions, immunohistochemical staining of Ly6G was performed. Ly6G$^+$ neutrophils were located in both the atherosclerotic plaques in the aortic sinus, as well as in lesions of the aortic arch (Figure 5C and 5D). The number of neutrophils per plaque area was increased at 4 and 8 weeks of HFD in the aortic root and was lower at 12 weeks of HFD. In the aortic arch, the number of neutrophils peaked at 4 weeks of HFD, followed by a decline in the further course of the study. Frequencies of neutrophils were higher in the aortic arch region compared with the aortic root (Figure 5A and 5B).

Discussion

Inflammatory processes are driving forces of atherosclerotic plaque development. Monocyte recruitment and macrophage differentiation, as well as the uptake of modified low-density lipoproteins by macrophages, lead to signaling cascades that result in the expression and release of chemokines, proinflammatory cytokines, and proteases attracting other inflammatory cells to stimulate the inflammatory process.[23] In recent years, also neutrophils have been revealed to support early atherosclerotic plaque development.[5] Neutrophils can prime monocyte recruitment.[12] Moreover, neutrophil extracellular traps that are released by neutrophils that undergo a specific cell death and consist of decondensed chromatin containing neutrophil elastase and myeloperoxidase[24] can be found within arteries of atherosclerotic mice.[25] Investigating the interplay between macrophages and neutrophils, neutrophil extracellular traps were shown to prime macrophages for cytokine release, boosting the inflammatory process and promoting atherosclerotic lesion formation.[26]

The possibility of tracking early events in atherosclerotic lesion formation in vivo would not only offer novel insight into the pathogenesis of atherosclerosis but also enable the assessment of pharmacological interventions targeting atherosclerosis at a stage that is at least partially reversible. To evaluate the potential of molecular imaging during early stages of atherosclerosis, we assessed the performance of an elastase-targeting near-infrared imaging agent to capture elastase activity noninvasively and in vivo.

It has previously been shown by Kossodo et al that the probe used in our study is preferentially cleared and rapidly activated by neutrophil elastase (both in mice and humans) and is resistant to other serine proteases.[27] We have confirmed that the elastase-targeted NIRF imaging agent showed a dose-dependent activation by proteases secreted after isolation and stimulation of both murine and human neutrophils. The specificity of the probe was tested by conducting inhibition experiments with sivelestat. Sivelestat is a selective inhibitor of murine and human elastase and is clinically used in acute lung injury.[28] Sivelestat inhibited human neutrophil elastase with a half maximal inhibitory concentration value comparable to published data.[20] Mouse elastase inhibition with sivelestat was more powerful compared with inhibition of human elastase.

After successful evaluation of the NIRF probe ex vivo, we subsequently studied the probe performance in vivo in a murine model of atherosclerosis.

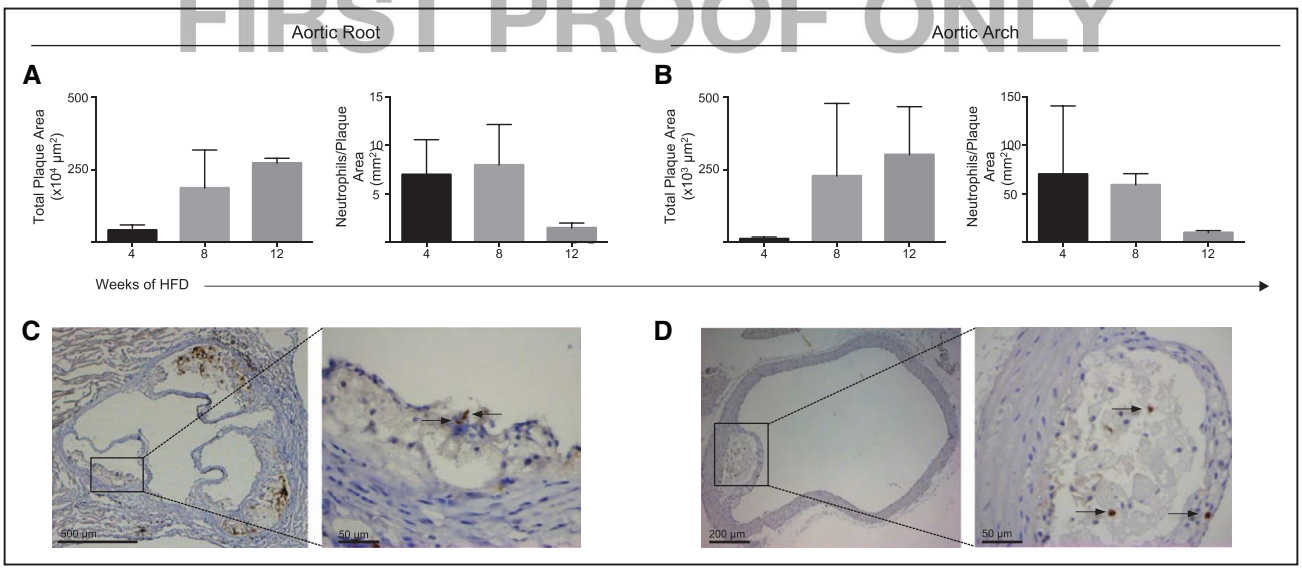

Figure 5. Detection of neutrophils in atherosclerotic plaques. **A** and **B**, Quantification of total plaque area and number of neutrophils/plaque area in aortic root sections (**A**) and aortic arch sections (**B**). Graph shows mean±SD (4 weeks of high-fat diet [HFD], n=3; 8 weeks of HFD, n=3; 12 weeks of HFD, n=3). **C** and **D**, Representative immunostaining of Ly6G-positive neutrophils (indicated by arrows) in sections of the aortic root (**C**) and aortic arch (**D**). The cells are counterstained with hematoxylin, showing cell nuclei in blue.

FMT-XCT as a noninvasive imaging approach allows the detection of protease activity in vivo. The assessed probe was recently investigated in a mouse model of acute lung injury,[19] in a tumor mouse model with neutrophil elastase activity,[29] and in chlamydia-associated inflammation.[30] In our study, we measured the fluorescent signal in vivo by hybrid FMT-XCT, which enabled the anatomic localization of the targeted fluorescence to regions of the aortic root and arch of atherosclerotic mice. The measured fluorescence increased at 4 weeks of HFD and slightly declined again at 8 and 12 weeks of HFD. These NIRF signals generated by the neutrophil elastase 680 probe appear large and diffuse because of scattering in the biological tissue so that reconstruction of a high-resolution image with FMT-XCT is difficult, in line with previous reports.[31–34]

Ex vivo experiments of whole-body cryoslicing corroborated the in vivo results and confirmed increased fluorescence signals originating from the aortic wall, and quantification of cryoslicing results similarly showed an increased fluorescence signal at 4 and 8 weeks, thus, at early stages of lesion development.

Fluorescence ratios were calculated to evaluate the fluorescence signal in cryosections in between mice. Because of distinct integration times of the camera as a result of slight changes of the laser light direction relative to the region of interest, its distance to the camera, and so forth, there were differences in the dynamic range of fluorescence in each mouse, even after reducing background effects, so that the fluorescence ratio was calculated for quantitative comparison. Higher variability of the fluorescence ratio at 8 and 12 weeks may have been caused by difficulties of manual segmentation in the region of interest (close to the aorta) because of its small size and relative low signal intensity, whereas the same is not a problem with FMT-XCT data. FMT-XCT data offer a more accurate localization of the aorta because of better anatomic information of the XCT. Manual segmentation of the region of interest is also less difficult at 4 weeks of HFD because the signal intensity in these mice is higher, associated with a much higher fluorescence ratio, hence, enabling a more accurate segmentation with lesser variability. However, it has to be conceded that spatial resolution of FMT remains limited. Scattering of emitted fluorescence from deep tissue results in a diffuse FMT signal, which may seem to extend the region of interest in the aortic arch, similar to previous findings.[31–34] In addition, the fluorescence signal observed in FMT-XCT imaging contains fluorescence emitted from the target, but also background autofluorescence, as well as fluorescence that may have been scattered from signals outside the blood vessel or adjacent mediastinal structures. Signals in the region of the aortic arch may, thus, not only originate from fluorescence emitted from plaque tissue but also from, for example, extravascular activation or trapping of the cleaved product. Those signals cannot be separated by FMT inversion. This may also be reflected by our FMT-XCT quantification results: at week 0, there is still a positive quantification value rather than zero, which may indicate the extent of autofluorescence and extravascular probe activation. However, signal intensities are much stronger in atherosclerotic mice at week 4, week 8, and week 12. This increase in fluorescence strongly indicates that despite the limitations in spatial resolution, elastase-targeted FMT-XCT imaging can be used for in vivo detection of early atherosclerosis.

Fluorescence microscopy additionally verified the presence of emitted fluorescence from the elastase targeting NIRF agent in the atherosclerotic aorta and regions of plaque formation. A major contribution of plaque autofluorescence was ruled out by investigating atherosclerotic mice not injected with the NIRF probe, which did not show any fluorescence. These results, thus, demonstrate that the measured elastase activity is primarily associated with early-stage atherosclerotic lesions.

Immunofluorescence staining and histological analyses were conducted to assess the number and localization of intralesional neutrophils. The number of neutrophils per plaque area was increased at 4 and 8 weeks after initiation of HFD and decreased thereafter, in accordance with previously described kinetics.[4,18] The relative number of neutrophils corresponded to the results of elastase activity determined by FMT-XCT in vivo and by cryosection analysis ex vivo. Correlation analyses of cell numbers with fluorescence signals of all mice fed a HFD in vivo, however, did not reveal a significant correlation. It should be noted, however, that neutrophil counts within plaque tissue are low (≈5 neutrophils per square millimeter of plaque), so that it is unlikely that living neutrophils are solely responsible for the elastase fluorescence signal. Lin et al[15] conducted an FMT imaging study with atherosclerotic mice using cathepsin and $\alpha_v\beta_3$ integrin NIRF agents. The minimum macrophage cell count was around 100 for correlation to the FMT signal. However, neutrophils have a short life span, so that low numbers visualized by histology may not necessarily correspond to the total number of recruited neutrophils. In addition, neutrophils contain preformed granules containing different effector molecules, such as neutrophil elastase. These may be released and deposited within the artery[35,36] and may persist even after neutrophil cell death. Similarly, elastase-containing neutrophil extracellular traps can be found within the arterial wall.[26] In line, in some cases, we could clearly colocalize the fluorescence signal of the elastase NIRF probe to specific cells with segmented nuclear morphology typical for neutrophils and Ly6G staining, whereas we were also able to detect staining of the NIRF probe in plaque regions without colocalization with Ly6G. This may have been caused by the presence of elastase deposits still present after the donor neutrophil has died. Another explanation why a measurable fluorescent elastase signal can be detected despite low numbers of neutrophils is that neutrophil elastase may also be derived from alternative sources. Dollery et al[13] showed that activated vascular endothelial cells, monocytes, and macrophages contain neutrophil elastase mRNA and can produce neutrophil elastase. Thus, endothelial cells themselves and early infiltrating mononuclear phagocytes may in addition contribute to lesional elastase activity. In addition, it could also be possible that other enzymes contribute to the fluorescent signal by unspecific cleavage of the amino acid sequence of the NIRF agent. Potential protease substrate cleavage sites can be predicted using a published online tool.[37] This indicated potential substrate cleavage also by matrix metalloproteinases 9

and cathepsin G for the amino acid sequence of the assessed probe, which needs to be investigated in future experiments.

The key advantage of molecular imaging is the ability to track inflammatory processes noninvasively. Nahrendorf et al[14] successfully tested different NIRF agents specific for proteases in atherosclerotic lesion. In addition, integrin-targeted FMT imaging offered new insights as a molecular imaging tool of atherosclerosis.[15] Besides FMT, also magnetic resonance imaging may constitute a preclinical imaging approach focusing on enzyme-sensitive magnetic resonance agents. Myeloperoxidase, secreted predominantly by neutrophils, plays a central role in plaque, destabilizing at later stages of atherosclerosis. The study conducted by Ronald et al[38] showed myeloperoxidase activity using a myeloperoxidase magnetic resonance sensor in atherosclerotic rabbits noninvasively. These studies, however, uniformly addressed later stages of atherosclerosis.

Early-stage atherosclerosis may still be reversible to a certain degree. Sivelestat, a synthetic neutrophil elastase inhibitor, effectively reduced inflammation in acute lung injury in animal models and clinical trials.[28,39] However, sivelestat has not been investigated in the context of atherosclerosis. Taking recent work by Warnatsch et al[26] and our results into account, the presence of neutrophil elastase in early atherosclerotic lesions may suggest its suitability for pharmacological intervention. Likewise, pharmacological interventions suppressing the early progression of atherosclerosis could potentially be monitored in vivo by detecting elastase activity.

Although fluorescence molecular imaging has long been restricted to preclinical setups, its clinical translation is within reach. Miniaturization of fluorescence detectors has enabled mounting the entire instrumentation of angiography catheters, already evaluated successfully in large animal models of atherosclerosis.[40,41] Detection of early atherosclerotic lesions in patients before calcifications occur is limited using current technologies of biomedical imaging. Detection of neutrophil elastase using catheter-based fluorescence imaging would enable to capture early lesion formation also in patients, thereby, enabling tailored treatment approaches. Similarly, because elastase plays an import role during plaque rupture, catheter-guided detection of vulnerable atherosclerotic lesions might become feasible in the clinical setting.

In summary, the present study provides new insights into elastase-targeted imaging of early stages of atherosclerosis. Our findings show that the assessed probe can be used as a fluorescent biomarker of elastase activity in atherosclerotic mouse models. This specific imaging approach could, thus, be explored for application in a clinical setting for earlier diagnosis and treatment of atherosclerosis.

Acknowledgments

We thank Sarah Glasl and Melanie Schott for excellent technical assistance.

Sources of Funding

This work was supported by Alexander von Humboldt Postdoctoral Fellowship program to J. Prakash, by the Deutsche Forschungsgemeinschaft (WI3686/4-1 to M. Wildgruber and SFB688 TPA22 to A. Zernecke) and the TUM International Graduate School of Science and Engineering (IGSSE) to A. Glinzer, M. Thon, M. Gee, A. Zernecke, and M. Wildgruber (Project AMMA).

Disclosures

None.

References

1. Cannon B. Cardiovascular disease: biochemistry to behaviour. *Nature*. 2013;493:S2–S3. doi: 10.1038/493S2a.
2. Hansson GK. Inflammation, atherosclerosis, and coronary artery disease. *N Engl J Med*. 2005;352:1685–1695. doi: 10.1056/NEJMra043430.
3. Dahlöf B. Cardiovascular disease risk factors: epidemiology and risk assessment. *Am J Cardiol*. 2010;105(1 suppl):3A–9A. doi: 10.1016/j.amjcard.2009.10.007.
4. van Leeuwen M, Gijbels MJ, Duijvestijn A, Smook M, van de Gaar MJ, Heeringa P, de Winther MP, Tervaert JW. Accumulation of myeloperoxidase-positive neutrophils in atherosclerotic lesions in LDLR$^{-/-}$ mice. *Arterioscler Thromb Vasc Biol*. 2008;28:84–89. doi: 10.1161/ATVBAHA.107.154807.
5. Zernecke A, Bot I, Djalali-Talab Y, Shagdarsuren E, Bidzhekov K, Meiler S, Krohn R, Schober A, Sperandio M, Soehnlein O, Bornemann J, Tacke F, Biessen EA, Weber C. Protective role of CXC receptor 4/CXC ligand 12 unveils the importance of neutrophils in atherosclerosis. *Circ Res*. 2008;102:209–217. doi: 10.1161/CIRCRESAHA.107.160697.
6. Naruko T, Ueda M, Haze K, van der Wal AC, van der Loos CM, Itoh A, Komatsu R, Ikura Y, Ogami M, Shimada Y, Ehara S, Yoshiyama M, Takeuchi K, Yoshikawa J, Becker AE. Neutrophil infiltration of culprit lesions in acute coronary syndromes. *Circulation*. 2002;106:2894–2900.
7. Rotzius P, Thams S, Soehnlein O, Kenne E, Tseng CN, Björkström NK, Malmberg KJ, Lindbom L, Eriksson EE. Distinct infiltration of neutrophils in lesion shoulders in ApoE-/- mice. *Am J Pathol*. 2010;177:493–500. doi: 10.2353/ajpath.2010.090480.
8. Nathan C. Neutrophils and immunity: challenges and opportunities. *Nat Rev Immunol*. 2006;6:173–182. doi: 10.1038/nri1785.
9. Eades-Perner AM, Thompson J, van der Putten H, Zimmermann W. Mice transgenic for the human CGM6 gene express its product, the granulocyte marker CD66b, exclusively in granulocytes. *Blood*. 1998;91:663–672.
10. Ionita MG, van den Borne P, Catanzariti LM, Moll FL, de Vries JP, Pasterkamp G, Vink A, de Kleijn DP. High neutrophil numbers in human carotid atherosclerotic plaques are associated with characteristics of rupture-prone lesions. *Arterioscler Thromb Vasc Biol*. 2010;30:1842–1848. doi: 10.1161/ATVBAHA.110.209296.
11. Daley JM, Thomay AA, Connolly MD, Reichner JS, Albina JE. Use of Ly6G-specific monoclonal antibody to deplete neutrophils in mice. *J Leukoc Biol*. 2008;83:64–70. doi: 10.1189/jlb.0407247.
12. Soehnlein O, Zernecke A, Eriksson EE, Rothfuchs AG, Pham CT, Herwald H, Bidzhekov K, Rottenberg ME, Weber C, Lindbom L. Neutrophil secretion products pave the way for inflammatory monocytes. *Blood*. 2008;112:1461–1471. doi: 10.1182/blood-2008-02-139634.
13. Dollery CM, Owen CA, Sukhova GK, Krettek A, Shapiro SD, Libby P. Neutrophil elastase in human atherosclerotic plaques: production by macrophages. *Circulation*. 2003;107:2829–2836. doi: 10.1161/01.CIR.0000072792.65250.4A.
14. Nahrendorf M, Waterman P, Thurber G, Groves K, Rajopadhye M, Panizzi P, Marinelli B, Aikawa E, Pittet MJ, Swirski FK, Weissleder R. Hybrid *in vivo* FMT-CT imaging of protease activity in atherosclerosis with customized nanosensors. *Arterioscler Thromb Vasc Biol*. 2009;29:1444–1451. doi: 10.1161/ATVBAHA.109.193086.
15. Lin SA, Patel M, Suresch D, Connolly B, Bao B, Groves K, Rajopadhye M, Peterson JD, Klimas M, Sur C, Bednar B. Quantitative longitudinal imaging of vascular inflammation and treatment by ezetimibe in apoE mice by FMT using new optical imaging biomarkers of cathepsin activity and α(v)β(3) integrin. *Int J Mol Imaging*. 2012;2012:189254. doi: 10.1155/2012/189254.
16. Nahrendorf M, Sosnovik DE, Waterman P, Swirski FK, Pande AN, Aikawa E, Figueiredo JL, Pittet MJ, Weissleder R. Dual channel optical tomographic imaging of leukocyte recruitment and protease activity in the healing myocardial infarct. *Circ Res*. 2007;100:1218–1225. doi: 10.1161/01.RES.0000265064.46075.31.
17. Galli SJ, Borregaard N, Wynn TA. Phenotypic and functional plasticity of cells of innate immunity: macrophages, mast cells and neutrophils. *Nat Immunol*. 2011;12:1035–1044. doi: 10.1038/ni.2109.

18. Drechsler M, Megens RT, van Zandvoort M, Weber C, Soehnlein O. Hyperlipidemia-triggered neutrophilia promotes early atherosclerosis. *Circulation*. 2010;122:1837–1845. doi: 10.1161/CIRCULATIONAHA.110.961714.
19. Kossodo S, Zhang J, Groves K, Cuneo GJ, Handy E, Morin J, Delaney J, Yared W, Rajopadhye M, Peterson JD. Noninvasive *in vivo* quantification of neutrophil elastase activity in acute experimental mouse lung injury. *Int J Mol Imaging*. 2011;2011:581406. doi: 10.1155/2011/581406.
20. Kawabata K, Suzuki M, Sugitani M, Imaki K, Toda M, Miyamoto T. ONO-5046, a novel inhibitor of human neutrophil elastase. *Biochem Biophys Res Commun*. 1991;177:814–820.
21. Ishibashi S, Goldstein JL, Brown MS, Herz J, Burns DK. Massive xanthomatosis and atherosclerosis in cholesterol-fed low density lipoprotein receptor-negative mice. *J Clin Invest*. 1994;93:1885–1893. doi: 10.1172/JCI117179.
22. Whitman SC. A practical approach to using mice in atherosclerosis research. *Clin Biochem Rev*. 2004;25:81–93.
23. Hansson GK, Hermansson A. The immune system in atherosclerosis. *Nat Immunol*. 2011;12:204–212. doi: 10.1038/ni.2001.
24. Papayannopoulos V, Metzler KD, Hakkim A, Zychlinsky A. Neutrophil elastase and myeloperoxidase regulate the formation of neutrophil extracellular traps. *J Cell Biol*. 2010;191:677–691. doi: 10.1083/jcb.201006052.
25. Megens RT, Vijayan S, Lievens D, Döring Y, van Zandvoort MA, Grommes J, Weber C, Soehnlein O. Presence of luminal neutrophil extracellular traps in atherosclerosis. *Thromb Haemost*. 2012;107:597–598. doi: 10.1160/TH11-09-0650.
26. Warnatsch A, Ioannou M, Wang Q, Papayannopoulos V. Inflammation. Neutrophil extracellular traps license macrophages for cytokine production in atherosclerosis. *Science*. 2015;349:316–320. doi: 10.1126/science.aaa8064.
27. Kalupov T, Brillard-Bourdet M, Dadé S, Serrano H, Wartelle J, Guyot N, Juliano L, Moreau T, Belaaouaj A, Gauthier F. Structural characterization of mouse neutrophil serine proteases and identification of their substrate specificities: relevance to mouse models of human inflammatory diseases. *J Biol Chem*. 2009;284:34084–34091. doi: 10.1074/jbc.M109.042903.
28. Zeiher BG, Matsuoka S, Kawabata K, Repine JE. Neutrophil elastase and acute lung injury: prospects for sivelestat and other neutrophil elastase inhibitors as therapeutics. *Crit Care Med*. 2002;30(5 suppl):S281–S287.
29. Mitra S, Modi KD, Foster TH. Enzyme-activatable imaging probe reveals enhanced neutrophil elastase activity in tumors following photodynamic therapy. *J Biomed Opt*. 2013;18:101314. doi: 10.1117/1.JBO.18.10.101314.
30. Patel M, Lin SA, Boddicker MA, DeMaula C, Connolly B, Bednar B, Heinrichs JH, Smith JG. Quantitative in vivo detection of Chlamydia muridarum associated inflammation in a mouse model using optical imaging. *Mediators Inflamm*. 2015;2015:264897. doi: 10.1155/2015/264897.
31. Ale A, Ermolayev V, Herzog E, Cohrs C, de Angelis MH, Ntziachristos V. FMT-XCT: *in vivo* animal studies with hybrid fluorescence molecular tomography-X-ray computed tomography. *Nat Methods*. 2012;9:615–620. doi: 10.1038/nmeth.2014.
32. Simon RA, John CS. Optical tomography: forward and inverse problems. *Inverse Problems*. 2009;25:123010.
33. Zhang G, Liu F, Zhang B, He Y, Luo J, Bai J. Imaging of pharmacokinetic rates of indocyanine green in mouse liver with a hybrid fluorescence molecular tomography/x-ray computed tomography system. *J Biomed Opt*. 2013;18:040505. doi: 10.1117/1.JBO.18.4.040505.
34. Haller J, Hyde D, Deliolanis N, de Kleine R, Niedre M, Ntziachristos V. Visualization of pulmonary inflammation using noninvasive fluorescence molecular imaging. *J Appl Physiol (1985)*. 2008;104:795–802. doi: 10.1152/japplphysiol.00959.2007.
35. Soehnlein O. Multiple roles for neutrophils in atherosclerosis. *Circ Res*. 2012;110:875–888. doi: 10.1161/CIRCRESAHA.111.257535.
36. Alfaidi M, Wilson H, Daigneault M, Burnett A, Ridger V, Chamberlain J, Francis S. Neutrophil elastase promotes interleukin-1β secretion from human coronary endothelium. *J Biol Chem*. 2015;290:24067–24078. doi: 10.1074/jbc.M115.659029.
37. Song J, Tan H, Perry AJ, Akutsu T, Webb GI, Whisstock JC, Pike RN. PROSPER: an integrated feature-based tool for predicting protease substrate cleavage sites. *PLoS One*. 2012;7:e50300. doi: 10.1371/journal.pone.0050300.
38. Ronald JA, Chen JW, Chen Y, Hamilton AM, Rodriguez E, Reynolds F, Hegele RA, Rogers KA, Querol M, Bogdanov A, Weissleder R, Rutt BK. Enzyme-sensitive magnetic resonance imaging targeting myeloperoxidase identifies active inflammation in experimental rabbit atherosclerotic plaques. *Circulation*. 2009;120:592–599. doi: 10.1161/CIRCULATIONAHA.108.813998.
39. Zeiher BG, Artigas A, Vincent JL, Dmitrienko A, Jackson K, Thompson BT, Bernard G; STRIVE Study Group. Neutrophil elastase inhibition in acute lung injury: results of the STRIVE study. *Crit Care Med*. 2004;32:1695–1702.
40. Jaffer FA, Calfon MA, Rosenthal A, Mallas G, Razansky RN, Mauskapf A, Weissleder R, Libby P, Ntziachristos V. Two-dimensional intravascular near-infrared fluorescence molecular imaging of inflammation in atherosclerosis and stent-induced vascular injury. *J Am Coll Cardiol*. 2011;57:2516–2526. doi: 10.1016/j.jacc.2011.02.036.
41. Yoo H, Kim JW, Shishkov M, Namati E, Morse T, Shubochkin R, McCarthy JR, Ntziachristos V, Bouma BE, Jaffer FA, Tearney GJ. Intra-arterial catheter for simultaneous microstructural and molecular imaging in vivo. *Nat Med*. 2011;17:1680–1684. doi: 10.1038/nm.2555.

Highlights

- The elastase-targeted fluorescent agent Neutrophil Elastase 680 FAST is specifically cleaved and activated by activated neutrophils.
- In atherosclerosis-prone mice fed a Western-type diet, the elastase-targeting imaging probe can detect early atherosclerotic lesions in the aortic arch by hybrid fluorescence molecular tomography/x-ray computed tomography.
- Fluorescence molecular tomography/x-ray computed tomography–elicited signals were verified to locate to the aortic arch and to originate from the atherosclerotic arterial wall by whole-body cryoslicing and histology.
- These data highlight that elastase-targeted imaging can be used as a fluorescent biomarker of elastase activity to detect early atherosclerotic lesions.

Arteriosclerosis, Thrombosis, and Vascular Biology

JOURNAL OF THE AMERICAN HEART ASSOCIATION

Targeting Elastase for Molecular Imaging of Early Atherosclerotic Lesions

Almut Glinzer, Xiaopeng Ma, Jaya Prakash, Melanie A. Kimm, Fabian Lohöfer, Katja Kosanke, Jaroslav Pelisek, Moritz P. Thon, Sandra Vorlova, Katrin G. Heinze, Hans-Henning Eckstein, Michael W. Gee, Vasilis Nitziachristos, Alma Zernecke and Moritz Wildgruber

Arterioscler Thromb Vasc Biol. published online December 29, 2016;
Arteriosclerosis, Thrombosis, and Vascular Biology is published by the American Heart Association, 7272 Greenville Avenue, Dallas, TX 75231

Print ISSN: 1079-5642. Online ISSN: 1524-4636

Material and Methods

Isolation of murine and human neutrophils

To isolate and purify neutrophils from mouse bone marrow, femur and tibiae of mice were removed. The end of the bones were cut off and flushed with a syringe with 1% bovine serum albumin in phosphate buffered saline. The cell suspension was passed through a 70 µm cell strainer. After centrifugation (500 g, 10 min) the cell pellet was resuspended in 1% bovine serum albumin in phosphate buffered saline. The cells were then layered over a density gradient of Histopaque®-1119 and Histopaque®-1077 (Sigma-Aldrich) and centrifuged (700 g, 30 min, without break). After collecting the neutrophils at the interface of both histopaque layers cells were washed and counted. Purity of neutrophils was assessed by flow cytometry using antibodies from BD biosciences (CD45 (APC-Cy7; Clone 30-F11); CD11b (V500; Clone M1/70); Ly6G (V450; Clone 1A8)). Cell suspensions were analyzed using a FACS Canto II flow cytometer (BD, Biosciences) and data were analyzed by FlowJo Software (Treestar Inc.). Human neutrophils were isolated from venous blood of healthy volunteers. To obtain neutrophil cell suspensions, whole blood was diluted 1:1 with phosphate buffered saline and layed over density gradients and processed as described above.

Imaging Agent

Neutrophil Elastase FAST 680 (Perkin Elmer, Waltham, Massachusetts) is a preclinical fluorescence imaging agent emitting light in the near infrared spectrum (excitation 675 nm / emission 693 nm). It consists of a dedicated peptide sequence (PMAVVQSVP) with two VivoTag-S680 fluorochromes, which are self-quenched and become highly fluorescent after cleavage by neutrophil elastase. Plasma half-life of the agent is 3 hours with renal clearance only[1].

In vitro activation of Neutrophil Elastase 680 FAST

Experiments were carried out in 96-well plates with black sides and bottom in 100 µl/well at 37°C. For dose-response experiments 50,000 cells/ml were lysed with 0.01% Triton X and incubated with different concentrations (0.5 µM - 10 µM) of Neutrophil Elastase 680 FAST. For cell stimulation, 50,000 cells/ml were treated with phorbol-12-myristate 13-acetate (PMA)/Ionomycin (0.5 µg/ml or 1 µg/ml; Sigma-

Aldrich) and N-Formyl-Met-Leu-Phe (fMLP, 10 µg/ml or 1 µg/ml, Sigma-Aldrich) and incubated with 5 µM Neutrophil Elastase FAST 680. For blocking experiments 50,000 cells/ml were lysed with 0.01% Triton X and incubated with different concentrations of the selective elastase inhibitor, sivelestat [2] (S7198, Sigma-Aldrich, St.Louis, USA) ranging from 0.01 nM - 2000 nM for 30 min; thereafter the NIRF agent (5 µM) was added. The fluorescence intensity was measured over a time period of 90 min, and conducted at excitation/emission wavelengths of 663/690 nm using a fluorescence plate reader (TECAN infinite M1000 pro). To analyze probe cleavage kinetics, the Michaelis constant (K_m) was calculated using the Michaelis-Menten equation under consideration of determined reaction rates under different substrate concentrations, and IC_{50} values of sivelestat were determined.

Mouse model of atherosclerosis

LDL-receptor deficient mice (*LDLr⁻/⁻,* B6.129S7-Ldlrtm1Her/J, obtained from the Jackson Laboratory) were used. At the age of 14 to 15 weeks *LDLr⁻/⁻* mice were placed on a Western Type high fat diet (HFD, 21% fat, 0.15% cholesterol, 19.5% casein, Altromin, Lage, Germany) for a period of 4, 8 or 12 weeks before imaging by the FMT-XCT hybrid system. After imaging, mice were sacrificed for ex vivo analyses. All animal experiments were approved by local authorities (55.2.1.54-2532-115-13, Regierung von Oberbayern, München, Germany) in accordance with the German animal protection law.

In vivo imaging: Fluorescence Molecular Tomography-X-ray computed tomography (FMT-XCT)

For in vivo experiments, mice were imaged at 0 (n=10), 4 (n=10), 8 (n=8) and 12 (n=4) weeks of HFD. Before each imaging time point, the chest was shaved followed by chemically depilation as the fur is significantly absorbing and scattering the near-infrared fluorescence (NIRF) light. 100µL of Neutrophil Elastase 680 FAST was injected via tail vein injection (4 nmol/100µL). Imaging was performed at 4h post probe injection. Atherosclerotic mice that did not receive the imaging agent were used to determine the level of autofluorescence. To improve segmentation of the chest XCT images, an intravascular CT contrast agent (Exitron nano 12000, 100µl/25g mouse) was immediately injected before scanning. Mice were anesthetized by isoflurane inhalation (isoflurane 2.5 %, O_2 0.85 L/min) during the

imaging measurement. After finishing the experiments, mice were euthanized for further ex vivo analysis. All mice were imaged using a FMT-XCT hybrid imaging system [3, 4]. The system combines two imaging modalities, namely FMT and XCT, for imaging small animal disease models. Co-registered XCT images with high resolution can provide anatomical information for FMT, which improves the FMT three-dimensional functional and molecular reconstruction performance in a fundamental way [4]. For data acquisition, each mouse was first illuminated by a 680nm laser in a 360° trans-illumination mode. Excitation and emission images were both acquired at 20 equally spaced gantry locations by using a scientific charge-coupled device camera cooled at -80˚C with two different sets of filters placed in front of it (one for excitation and one for emission). Around 30 different positions of laser illumination in the region of interest were calculated automatically by first-acquired white light reference images at each gantry location. Furthermore, the mouse was scanned by using the integrated XCT system, which collected projections over a field of view of 360°. The current and energy of the x-ray tube was 450 μA and 80 kV. After FMT-XCT data acquisition, three-dimensional fluorophore distribution was reconstructed by using sparse linear equations and sparse least squares methods [5] and XCT anatomical information as prior.

Anatomical images were reconstructed by filtered back projection method and semi-automatically segmented based on the gray-scale slices. Different optical parameters (absorption coefficients and scattering coefficients) were assigned to different organs for every mouse. Then, FMT inversion was performed iteratively to locate the fluorescent distribution. To quantify and statistically analyze the FMT reconstruction, mean values of the region of interest of fluorescence intensities (around 5 slices, 1 mm interval) were calculated afterwards.

Whole-body Cryoslicing & Fluorescence Microscopy of Neutrophil Elastase FAST 680

After imaging, mice were sacrificed and whole-body cryoslicing was performed followed by fluorescence microscopy to investigate the localization of the fluorescence signal ex vivo. This method provides slice images in the same orientation (transverse plane) as FMT-XCT data acquisition showing anatomy and near-infrared reagent distribution. After each time point, mice (0 weeks of HFD, n=2; 4, 8, and 12 weeks of HFD, n= 3) were sacrificed and frozen at -80°C. For

cryoslicing, the mouse torso was embedded in a mixture of O.C.T. (Optimal Cutting Temperature) medium and India Ink. Cryoslice imaging of the mice was performed using a multispectral imaging system combined with a cryomicrotome (Leica) [6]. Transversal slices of the thorax 150 µm apart were acquired. After each slice a planar colored image and planar fluorescence image (excitation 680 nm) were taken using a filtered white light source and a sensitive charge-coupled camera. For detailed further analyses, cryoslices (20 µm thickness) of the ascending aorta and the aortic arch were placed on adhesive-glass slides (SuperFrost plus, Thermo Scientific), cell nuclei were counterstained with DAPI and embedded in ProLong Gold (ThermoScientific). Sections were imaged by fluorescence microscopy using appropriate filters (Cy5.5 filter and DAPI) or brightfield (Zeiss Axio Imager 2, Zeiss Zen analysis software). Additional 5 µm cryosections through the aortic root were obtained and incubated with Neutrophil Elastase FAST 680 for 15 minutes. Sections were washed and mounted using Vectashield with DAPI (Vector Laboratories), and immediately visualized using a Leica TCS SP5 confocal microscope (Leica Microsystems).

Immunofluorescence Staining and Histological Analysis

Immunofluorescense staining of neutrophils was performed using 5 µm cryosections through the aortic root. After fixation using 4% PFA (1 hour), slides were blocked (1% bovine serum albumin, 2% mouse, rabbit and horse serum, 0.1% TX100 in PBS; Sigma Aldrich), and incubated with primary anti-Ly6G antibody (rat-anti mouse Ly6G, Clone 1A8, 1:200 dilution, BD), and secondary detection performed using anti-rat Alexa Fluor 488-conjugated goat-anti-rat antibody. Sections were coverslipped using Vectorshield mounint medium with DAPI. The extent of atherosclerosis and neutrophil counts in atherosclerotic lesions were evaluated by immunohistological methods. After in vivo imaging, mice (4, 8, and 12 weeks of HFD, n= 3) were euthanized and the heart and aortic arch were perfusion-fixed with phosphate buffered saline and 4% formalin. After the dehydrating process the aortic root and aortic arch was embedded in paraffin. Sectioned in the transverse plane (2.5 µm thickness, 25 µm apart) were placed on adhesive-glass slides, and neutrophil staining was performed using anti-Ly6G antibody (rat-anti mouse Ly6G, Clone 1A8, 1:200 dilution, BD). Following primary antibody incubation, neutrophils were visualized with the Dako Labeled Streptavidin-Biotin System, Horseradish

Peroxidase (LSAB System, HRP). A nuclei counterstain was performed with haematoxylin. The slides were analyzed by counting the number of neutrophils using a brightfield microscope (Leica Leica DM 4000 B) and measuring the plaque size using ImageJ software.

Statistics

Data are represented as mean ± SD. Comparisons over time were analyzed by one-way Analysis of Variance (ANOVA) followed by Bonferroni post-tests for multiple comparisons using GraphPad Prism Software 6.0. Differences with p-values < 0.05 were considered to be statistically significant.

References

1. Kossodo S, Zhang J, Groves K, Cuneo GJ, Handy E, Morin J, Delaney J, Yared W, Rajopadhye M, Peterson JD. Noninvasive in vivo quantification of neutrophil elastase activity in acute experimental mouse lung injury. *Int J Mol Imaging*. 2011;2011:581406
2. Kawabata K, Suzuki M, Sugitani M, Imaki K, Toda M, Miyamoto T. Ono-5046, a novel inhibitor of human neutrophil elastase. *Biochemical and Biophysical Research Communications*. 1991;177:814-820
3. Ale A, Ermolayev V, Herzog E, Cohrs C, de Angelis MH, Ntziachristos V. Fmt-xct: In vivo animal studies with hybrid fluorescence molecular tomography-x-ray computed tomography. *Nat Meth*. 2012;9:615-620
4. Schulz RB, Ale A, Sarantopoulos A, Freyer M, Soehngen E, Zientkowska M, Ntziachristos V. Hybrid system for simultaneous fluorescence and x-ray computed tomography. *IEEE Trans Med Imaging*. 2010;29:465-473
5. Paige CC, Saunders MA. Lsqr: An algorithm for sparse linear equations and sparse least squares. *ACM Trans. Math. Softw.* 1982;8:43-71
6. Sarantopoulos A, Themelis G, Ntziachristos V. Imaging the bio-distribution of fluorescent probes using multispectral epi-illumination cryoslicing imaging. *Mol Imaging Biol*. 2011;13:874-885